
Learning Robust Node Representations on Graphs

Xu Chen^{1,2}, Ya Zhang¹, Ivor Tsang², and Yuangang Pan²

¹Shanghai Jiao Tong University

{xuchen2016, ya_zhang}@sjtu.edu.cn

²University of Technology, Sydney

ivor.tsang@uts.edu.au, Yuangang.pan@uts.edu.au

Abstract

Graph neural networks (GNN), as a popular methodology for node representation learning on graphs, currently mainly focus on preserving the *smoothness* and *identifiability* of node representations. A robust node representation on graphs should further hold the *stability* property which means a node representation is resistant to slight perturbations on the input. In this paper, we introduce the *stability* of node representations in addition to the *smoothness* and *identifiability*, and develop a novel method called contrastive graph neural networks (CGNN) that learns robust node representations in an unsupervised manner. Specifically, CGNN maintains the *stability* and *identifiability* by a contrastive learning objective, while preserving the *smoothness* with existing GNN models. Furthermore, the proposed method is a generic framework that can be equipped with many other backbone models (e.g. GCN, GraphSage and GAT). Extensive experiments on four benchmarks under both transductive and inductive learning setups demonstrate the effectiveness of our method in comparison with recent supervised and unsupervised models.

1 Introduction

Graph Neural Networks (GNN) have recently become one crucial technique for node representation learning on graphs and has shown great promise for a variety of tasks with graph structured data Tang et al. [2016], Kipf and Welling [2017], Wang et al. [2018, 2019b], Li et al. [2019b]. Earliest work on GNN starts with ChebNet Defferrard et al. [2016], which introduces a fast localized convolution approach on graphs in spectral domain. The spectral convolution is further developed into spatial graph convolution such as GCN Kipf and Welling [2017], GraphSage Hamilton et al. [2017], GAT Veličković et al. [2018] and GraphHeat Xu et al. [2019]. These methods mainly focus on enforcing the *smoothness* and *identifiability* properties of node representations. The *smoothness* means connected nodes on graphs have local structures and their representations should be similar in the embedding space Kipf and Welling [2017], Hamilton et al. [2017], Veličković et al. [2019]. The *identifiability* indicates node representations from different structures are distinguishable from each other. While *smoothness* and *identifiability* have proved essential in node representation learning on graphs, another necessary property for robust node representations is *stability*, especially for noisy graph structured data Zhuang and Ma [2018], Zhang et al. [2019]. Without enforcing stability, most GNN methods would be sensitive to the slight perturbations of graphs and suffer from high variance Verma and Zhang [2019], Rong et al. [2019], Zhang et al. [2019] and thus lead to a non-robust feature estimator Verma and Zhang [2019], Saad et al. [2011], Hubbell et al. [2002]. An example to illustrate the *smoothness*, *identifiability* and *stability* is shown in Figure 1.

In this paper, we attempt to simultaneously enforce the three properties, i.e. *smoothness*, *identifiability*, and *stability*, and propose a novel method called contrastive graph neural networks for robust node

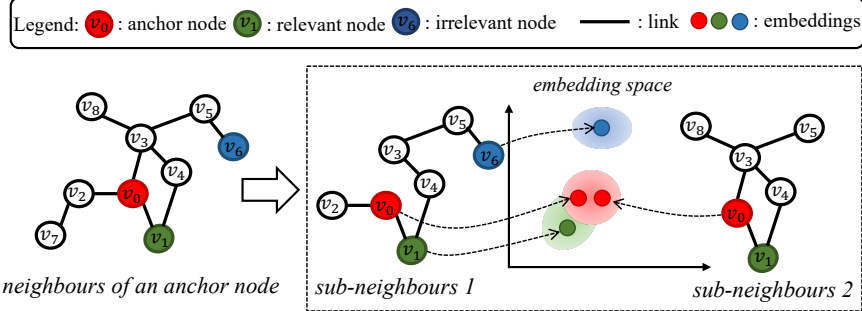


Figure 1: An example to illustrate the *smoothness*, *identifiability* and *stability* of node representations on graphs. For the anchor node v_0 , v_1 is a relevant node and v_6 is an irrelevant node. Here, we use different sub-neighbours to represent the slightly changed neighbours of the anchor node. A robust node representation should preserve the *smoothness* (i.e. v_0 and v_1 are close in the embedding space), the *identifiability* (i.e. v_0 and v_6 are distant from each other) and the *stability* (i.e. the representation of v_0 is stable to slight perturbations on the neighbours).

representation learning in an unsupervised manner. In CGNN, the *smoothness* is maintained by a GNN model that works as the feature extractor. The *identifiability* and *stability* are preserved by a contrastive learning objective. The contrastive learning objective estimates high similarity for representations of the same node with different perturbations and low similarity for representations of different nodes. More importantly, the proposed method is generic and can be equipped with different GNN backbones such as GCN, GraphSage and GAT. We show that the proposed method has better performance compared to other supervised and unsupervised GNN models on four benchmarks under both transductive and inductive learning setups. The contributions are summarized as follows:

- We propose that a robust node representation on graphs should preserve *stability*, in addition to *smoothness* and *identifiability*. Then we further develop a novel method called contrastive graph neural networks (CGNN) based on contrastive learning. CGNN learns more robust node representations in an unsupervised manner. Moreover, it is generic and can be equipped with many popular GNN backbone models for boosted performance.
- We conduct extensive experiments on four benchmarks under both transductive and inductive learning setups. The results demonstrate the effectiveness of our method in comparison with recent supervised and unsupervised GNN models.

2 Related Work

Recent progress of node representation learning by graph neural networks mainly concentrates on various convolutional techniques and advanced learning schemes.

Convolutional Techniques: Inspired by the success of convolution on images in Euclidean space, a number of researchers have tried to define the convolution on graphs in non-Euclidean space. In ChebNet Defferrard et al. [2016], a fast and localized convolution filter is defined on graphs in spectral domain. Then, Kipf et.al proposed graph convolutional networks (GCN) Kipf and Welling [2017] which utilizes a localized first-order approximation of the convolution in ChebNet. GCN is successfully applied in semi-supervised node classification and also associates graph convolution in spectral domain to that in spatial domain. Ying et.al Ying et al. [2018] defined the convolution on graphs with different neighborhood aggregation functions (e.g. ‘mean’, ‘max-pooling’ and ‘LSTM’) and proposed GraphSage which supports inductive learning on large-scale graphs. Recently, some works NT and Maehara [2019], Li et al. [2019c] reveal that the above graph convolution operations on graphs is a low-pass filter which emphasizes low-frequency signals (i.e. useful information) and suppresses high-frequency signals (i.e. noise). Following this, GraphHeat Xu et al. [2019] is proposed to enhance the low-pass filtering property by heat kernel Chung and Graham [1997]. In addition, Petar et.al Wang et al. [2019b] introduced attention mechanism to GNN and proposed graph attention networks (GAT).

Learning Schemes: The above GNN methods focusing on defining different convolution functions have achieved huge success in many applications Wang et al. [2018, 2019b], Li et al. [2019b]. However, the graph data may contain noise and the supervised labels are hard to obtain because of

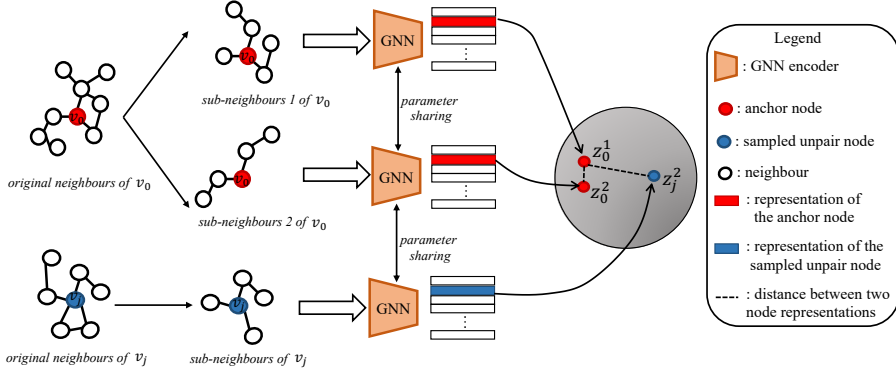


Figure 2: The framework of our contrastive graph neural networks (CGNN).

expensive human labour, which would cause a severe over-fitting problem Rong et al. [2019], Li et al. [2019a], Wu et al. [2020], Xu et al. [2018]. This problem has been analyzed from several aspects in terms of network architecture and noise perturbation. From the aspect of network architecture, inspired by the residual connections in CNN He et al. [2016], Li et.al Li et al. [2019a] introduced residual connections in GCN and proposed ResGCN. Similarly, JKNet Xu et al. [2018] designs a jumping knowledge network which fuses the features from different network layers to relieve the over-fitting problem. From the aspect of noise perturbation, Dropout Hinton et al. [2012] is a widely used technique to alleviate over-fitting by randomly setting certain feature dimensions to zeros. Specially for GNN, Rong et.al Rong et al. [2019] proposed DropEdge, where the edges in graphs are randomly dropped with a certain ratio before graph convolutions. DropEdge generates different perturbations of the graph connections and acts as one data augmentation technique to alleviate the over-fitting problem during training. DGI Veličković et al. [2019] is proposed to maximize the mutual information between a node representation and the corresponding high-level graph representation by constructing perturbation graphs.

3 Contrastive Graph Neural Networks

The problem of node representation learning on graphs is formulated as follows. Given an undirected graph $\mathcal{G} = (\mathcal{V}, \mathcal{E})$, $\mathcal{V} = \{v_i | 1 \leq i \leq N\}$ represents the nodes in the graph and $\mathcal{E} = \{e_{ij} | 1 \leq i, j \leq N\}$ denotes their connections. $e_{ij} = 1$ indicates node i and node j are connected while $e_{ij} = 0$ means not. Usually, graph \mathcal{G} is represented by an extremely sparse adjacent matrix $A \in \mathbb{R}^{N \times N}$ where the values are binary. The goal of node representation learning on graphs is to represent nodes into representative embeddings that can be applied in other tasks such as node classification.

The proposed method learns robust node representations in terms of *smoothness*, *stability* and *identifiability*. In CGNN, the *smoothness* is guaranteed by popular GNN backbones such as GCN Kipf and Welling [2017], GraphSage Hamilton et al. [2017] and GAT Veličković et al. [2018]. The *stability* and *identifiability* of node representations are maintained by a contrastive learning objective.

3.1 Stability by Sampling Neighbours

To achieve the *stability*, an intuitive way is to enforce a node representation from the slightly changed input to be close with the true node representation. However, it is non-trivial to obtain the true node representation because the graph data may contain noise. Instead, we enforce the *stability* among representations of the same node but has different perturbations.

To clarify our method, given an arbitrary anchor node v_0 , we denote its original neighbours as \mathcal{N}_0 . In order to construct perturbations on the neighbours \mathcal{N}_0 , we randomly drop edges of \mathcal{N}_0 with ratio ρ . Let $p(\mathcal{N}_0, \rho)$ be the distribution of \mathcal{N}_0 with ρ . Enforcing the *stability* among multiple samples from $p(\mathcal{N}_0, \rho)$ in each step is computational-inefficient. Instead, we employ an equivalent manner which enforces the *stability* between every two random samples from $p(\mathcal{N}_0, \rho)$ in different steps. Then, if we denote \mathcal{N}_0^1 and \mathcal{N}_0^2 are two sub-neighbours of \mathcal{N}_0 , we have:

$$\mathcal{N}_0^1, \mathcal{N}_0^2 \sim p(\mathcal{N}_0, \rho) \quad (1)$$

where \mathcal{N}_0^1 and \mathcal{N}_0^2 is two different sub-neighbours since the random dropping are conducted in two independent procedures. Let f_θ be a GNN backbone that has the smoothing characteristic, we have:

$$z_0^1 = f_\theta(\mathcal{N}_0^1), z_0^2 = f_\theta(\mathcal{N}_0^2) \quad (2)$$

where z_0^1 and z_0^2 are the anchor node's representations from \mathcal{N}_0^1 and \mathcal{N}_0^2 , respectively.

3.2 Contrastive Loss for Stability and Identifiability

To preserve high similarity for representations of the same node with different perturbations, referred to as *stability*, and enforce low similarity for representations of different nodes, referred to as *identifiability*, we propose to use the contrastive loss for the design of CGNN. The general architecture of CGNN is shown in Figure 2. In particular, we denote (z_0^1, z_0^2) as a paired sample. If z_j^2 is a node representation not belonging to v_0 , then (z_0^1, z_j^2) is an unpaired sample. We consider normalized close signals from (z_0^1, z_0^2) and (z_0^1, z_j^2) by a contrastive objective shown in Eq. 3.

$$\mathcal{L}_1 = -\mathbb{E}_{\{z_0^1, z_0^2, z_j^2 | j=1\}} \left[\log \frac{h_\phi(z_0^1, z_0^2)}{\sum_{j=0}^K h_\phi(z_0^1, z_j^2)} \right] \quad (3)$$

where h_ϕ is a score function that is high for paired samples and low for unpaired samples. K indicates the sampling size of unpaired samples. Through the contrastive objective in Eq. 3, we push the paired representations z_0^1 and z_0^2 are closer than the unpaired representations z_0^1 and z_j^2 in the embedding space. Following Mnih and Kavukcuoglu [2013], Oord et al. [2018], Tian et al. [2019], we implement the score function as Eq. 4 from the exponential family.

$$h_\phi(z_0^1, z_0^2) = e^{z_0^{1T} z_0^2 / \tau} \quad (4)$$

where τ is a temperature to control the distribution of h_ϕ . Similarly, by substituting the anchor representation z_0^1 in Eq. 3 with z_0^2 , we have Eq. 5:

$$\mathcal{L}_2 = -\mathbb{E}_{\{z_0^2, z_0^1, z_j^1 | j=1\}} \left[\log \frac{h_\phi(z_0^2, z_0^1)}{\sum_{j=0}^K h_\phi(z_0^2, z_j^1)} \right] \quad (5)$$

By summing Eq. 3 and Eq. 5 up, we have our final contrastive objective function:

$$\min_{\theta} \mathcal{L} = \mathcal{L}_1 + \mathcal{L}_2 \quad (6)$$

where θ is the only parameter from the GNN backbone model.

The proposed contrastive objective function \mathcal{L} actually is an estimator that maximizes the mutual information between z_0^1 and z_0^2 . Based on Oord et al. [2018], Poole et al. [2019], we demonstrate it in Appendix C, showing that:

$$\mathcal{I}(z_0^1, z_0^2) \geq \log(K) - \mathcal{L} \quad (7)$$

where \mathcal{L} is the *lower bound* of $\mathcal{I}(z_0^1, z_0^2)$. The *lower bound* becomes tighter when K becomes larger. Minimizing \mathcal{L} indeed maximizes the mutual information between z_0^1 and z_0^2 towards a specific direction where the paired node representations are more similar or dependent than the unpaired ones.

3.3 Noise Contrastive Estimation for Approximation

The softmax operation in Eq. 3 and Eq. 5 is computational-inefficient especially when a large K is used. Following recent advances in Gutmann and Hyvärinen [2010], Mnih and Kavukcuoglu [2013], Tian et al. [2019], we employ noise contrastive estimation (NCE) to approximate the above softmax calculation. NCE is a convergent estimator to estimate unnormalized statistical models. The idea of NCE is to apply non-linear logistic regression to discriminate observed data and some artificially constructed noise samples Gutmann and Hyvärinen [2010]. To clarify NCE, for z_0^1 , we denote z_x^2 as a variable which could either be the paired representation z_0^2 or the unpaired representation z_j^2 . Then, we define a binary latent variable c that determines whether two node representations are paired ($c = 1$) or unpaired ($c = 0$). The probability of $c = 1$ can be written as Eq. 8. Details of this derivation is shown in Appendix A.

$$p(c = 1 | z_0^1, z_x^2) = \frac{p_d(z_x^2 | z_0^1)}{p_d(z_x^2 | z_0^1) + K p_n(z_x^2 | z_0^1)} \quad (8)$$

where $p_d(\cdot, \cdot)$ means the data distribution and $p_n(\cdot, \cdot)$ indicates the noise distribution. The noise distribution $p_n(\cdot | z_1^0) = 1/N$ since the noise samples are randomly sampled (i.e. a uniform distribution). We estimate this probability by replacing $p_d(z_2^0 | z_1^0)$ with our unnormalized model $h_\phi(z_0^1, z_x^2)$. The binary class variable c is Bernoulli-distributed so that the NCE version of \mathcal{L}_1 can be written as:

$$\mathcal{L}_{1-NCE} = -\mathbb{E}_{\{z_0^1, z_0^2, z_j^2\}_{j=1}^K} \left[\log(p(c=1|z_0^1, z_0^2)) + K \log(p(c=0|z_0^1, z_j^2)) \right] \quad (9)$$

Similarly, we can have the NCE version of \mathcal{L}_2 and \mathcal{L} as Eq. 10 and Eq. 11, respectively.

$$\mathcal{L}_{2-NCE} = -\mathbb{E}_{\{z_0^2, z_0^1, z_j^1\}_{j=1}^K} \left[\log(p(c=1|z_0^2, z_0^1)) + K \log(p(c=0|z_0^2, z_j^1)) \right] \quad (10)$$

$$\mathcal{L}_{NCE} = \mathcal{L}_{1-NCE} + \mathcal{L}_{2-NCE} \quad (11)$$

In order to perform a fast calculation, we take Eq. 11 as our final objective function. In this NCE approximation, representations of the same node with various neighbours are denoted as positive samples and representations of different nodes are regarded as negative samples. By discriminating the positive and negative samples, the NCE objective is trying to learn the common factors of different variants of the same node and recognize the irrelevant factors.

3.4 Acceleration Strategies for Training

DropEdge Sampling Strategy: If we denote the number of training epochs as T , the complexity for constructing various sub-neighbours of N nodes is $\mathcal{O}(NT)$. In our implementation, following DropEdge Rong et al. [2019], we randomly drop edges on the adjacent matrix A one time for each epoch and then feed the perturbational adjacent matrices A^1 and A^2 instead of \mathcal{N}_0^1 and \mathcal{N}_0^2 into the model training. Then the complexity for constructing various sub-neighbours of N nodes is reduced to $\mathcal{O}(T)$. By using the sampling strategy in DropEdge Rong et al. [2019], the edge dropping process is largely accelerated.

Memory Bank Strategy: In order to efficiently sample K noise samples for \mathcal{L}_{NCE} , we follow the memory bank strategy in Wu et al. [2018], Tian et al. [2019]. In particular, the latent features of all nodes are stored in memory and synchronously updated after each loss back propagation. With this manner, we can optimize our objective function \mathcal{L}_{NCE} on the fly. The concise steps of CGNN are illustrated in Appendix D.

3.5 Sampling Bias on Small Graphs

The NCE estimator is a low variance and high biased estimator which indicates that we usually needs a large sampling size K to obtain a tight *lower bound* Oord et al. [2018], Hjelm et al. [2018]. For an arbitrary node v_0 on graphs, since nodes in graphs are dependent, a large sampling size would lead to the risk of sampling similar representations of v_0 and thus construct wrong contrastive signals. Given a graph \mathcal{G} with N nodes, if we denote \mathcal{K} as the set of sampled unpaired nodes and \mathcal{M} as the set of nodes that have high similarity with v_0 in the latent space, we have the following proposition:

Proposition 1 *For an arbitrary node v_0 in \mathcal{G} , the risk of sampling similar nodes in \mathcal{K} satisfies $\mathcal{R} = \frac{|\mathcal{K} \cap \mathcal{M}|}{|\mathcal{K}|}$. We tend to have low risk when N is large and $|\mathcal{M}|$ is small.*

where $|\cdot|$ indicates the length of a set. Details of this proposition is shown in Appendix E. This proposition indicates that the contrastive loss in Eq. 11 would be optimized in a wrong direction when the dataset size is too small or the number of similar nodes of v_0 is too large.

3.6 Comparisons with Other Methods

Previous GNN methods are able to preserve the *smoothness* property Li et al. [2018, 2019c], NT and Maehara [2019]. For supervised GNN methods, the *identifiability* of node representations could be preserved by sufficient labels, which is hard to be achieved because of the expensive human labour. Instead, apart from *smoothness* and *identifiability*, the proposed method preserves the *stability* and learns robust node representations in an unsupervised manner. It is worthwhile to mention that although DropEdge Rong et al. [2019] conducted in supervised learning assigns the same label for a node's representation of different sub-neighbours, it does not impose explicit *stability* constraints on node representations and cannot guarantee the *stability*. Instead, CGNN exploits explicit objective to maintain the *stability* property.

Table 1: The statistics of four benchmarks.

	#nodes	#edges	#density	#classes	#features	#label rate	Train/Val/Test
Pubmed	19,717	44,324	0.01%	3	500	0.30%	60/500/1,000
Facebook	22,470	170,823	0.03%	4	4,714	0.35%	80/120/rest
Coauthor-CS	18,333	81,894	0.02%	15	6,805	1.60%	300/450/rest
Coauthor-Phy	34,493	247,962	0.02%	5	8,415	57.98%	20,000/5,000/rest

In addition, DGI is another unsupervised learning method on graphs based on mutual information maximization. DGI maximizes the mutual information between a node representation and the corresponding high-level graph representation. In this way, DGI tries to keep more high-order information of nodes and achieve better *smoothness*. Instead, CGNN maximizes the mutual information of representations of the same node with different perturbations. The contrastive objective of CGNN is proposed to maintain the *stability* and *identifiability*.

4 Experiments and Analysis

4.1 Dataset Description

We conduct the experiments on four benchmarks varying in graph types and sizes. Pubmed is a widely used citation network. Facebook Rozemberczki et al. [2019] is a web page dataset where nodes are official Facebook pages and the edges are mutual connections between sites. Coauthor-CS and Coauthor-Phy Shchur et al. [2018] are two coauthor datasets. Each dataset has raw node features and class labels so that we can perform the classification task on it. For Pubmed, Facebook and Coauthor-CS, we conduct the transductive learning where all nodes and their raw features are accessible during training. For Coauthor-Phy, we conduct the inductive learning which indicates the test nodes are not seen during training. For Pubmed, we follow the common data splits of semi-supervised learning in many works Kipf and Welling [2017], Veličković et al. [2019], Wang et al. [2019b]. For Facebook and Coauthor-CS, we follow the setting in Shchur et al. [2018] where 20 nodes of each class are the train set and 30 nodes of each class are the validation set and the rest is the test set. For Coauthor-Phy in inductive learning, we randomly sample 20,000 nodes as train set and 5,000 nodes as validation set and the rest as test set. The dataset statistics are shown in Table 1.

4.2 Experiment Setups

Baselines: We make the comparison of CGNN with the following baselines in terms of various convolution techniques including GCN Kipf and Welling [2017], JKNet Xu et al. [2018], GraphSage Hamilton et al. [2017] and GAT Wang et al. [2019b], and advanced learning schemes including ResGCN Li et al. [2019a], DropEdge Rong et al. [2019] and DGI Veličković et al. [2019]. Among the baselines, DGI shows the state-of-the-art unsupervised learning performance and the others are supervised methods.

Parameter Settings: We implement our method with Pytorch on a machine with one Nvidia-1080 GPU. For GCN, ResGCN, JKNet and DropEdge, we use the released codes from others Rong et al. [2019]. For GraphSage, GAT and DGI, we use the implementations from a famous GNN library DGL Wang et al. [2019a]. By following Veličković et al. [2018, 2019], we set 8 attention heads and each dimension is 8 for GAT and its variant methods (DropEdge(GAT), CGNN(GAT)). For DGI, we follow the original paper Veličković et al. [2019] with the latent dimension as 512. For other baselines, we set the dimension as 128 by following Rong et al. [2019]. For our method, the dimension is set as 128 which is the same as the backbones except GAT. The hyper-parameters of baselines are set according to the original papers. For the proposed method, we set the learning rate as 0.001 with 5,000 iterations. According to the performance on the validation set, we set the drop ratio $\rho = 0.3$, the temperature $\tau = 0.1$ and the sampling size $K = 1024$ for our method. Since both DGI and the proposed method are conducted in unsupervised learning, we train a one-layer linear classifier for evaluation by following Veličković et al. [2019]. For all methods, The best trained model is chosen for testing according to the performance on the validation set.

Table 2: The classification accuracy(%) on different benchmarks. The best value for supervised models is emphasized with underline. The best value for unsupervised models is emphasized in bold.

		Transductive	Inductive		
Method		Pubmed	Facebook	Coauthor-CS	Coauthor-Phy
Supervised	GCN	<u>79.20(±0.38)</u>	66.37(±0.24)	92.01(±0.14)	93.35(±0.02)
	ResGCN	77.74(±0.39)	67.69(±0.60)	92.84(±0.24)	95.88(±0.03)
	JKNet	77.84(±0.11)	68.09(±0.75)	92.76(±0.22)	95.56(±0.15)
	GraphSage	79.02(±0.31)	69.62(±0.38)	92.60(±0.16)	95.28(±0.16)
	GAT	78.71(±0.21)	<u>72.24(±0.07)</u>	91.23(±0.06)	93.96(±0.04)
	DropEdge(GCN)	78.82(±0.29)	66.10(±0.19)	92.12(±0.12)	93.32(±0.02)
	DropEdge(ResGCN)	77.52(±0.38)	67.30(±0.75)	<u>93.01(±0.16)</u>	<u>95.89(±0.04)</u>
	DropEdge(JKNet)	77.85(±0.16)	67.68(±0.54)	92.74(±0.20)	95.77(±0.02)
	DropEdge(GraphSage)	78.53(±0.31)	69.25(±0.30)	92.77(±0.08)	95.41(±0.30)
	DropEdge(GAT)	78.90(±0.30)	71.57(±0.21)	91.32(±0.14)	93.80(±0.13)
Unsupervised	DGI	79.24(±0.50)	69.53(±1.25)	91.41(±0.12)	93.26(±0.35)
	CGNN(GCN)	81.34(±0.54)	71.13(±0.16)	92.35(±0.27)	92.76(±0.10)
	CGNN(ResGCN)	77.34(±0.53)	71.21(±0.29)	92.01(±0.19)	93.43(±0.27)
	CGNN(JKNet)	80.82(±0.48)	68.77(±1.31)	91.48(±0.18)	92.82(±0.08)
	CGNN(GraphSage)	81.81(±0.20)	71.55(±0.48)	91.21(±0.24)	93.33(±0.02)
	CGNN(GAT)	80.93(±0.40)	78.39(±0.64)	90.14(±0.37)	92.34(±0.03)

4.3 Node Classification Performance

Following Veličković et al. [2019], we conduct the node classification task to make the comparison with different methods. The node classification results on different benchmarks are summarized in Table 2. In this table, we report the mean classification accuracy (with standard derivation) on the test nodes after 5 runs with different random seeds. From the table, we have the following observations.

The proposed method outperforms the state-of-the-art unsupervised model DGI and even exceeds the supervised models on several datasets. On Pubmed, CGNN(GCN) reaches a 2.10% gain over DGI and a 2.14% gain over GCN. On Facebook, the proposed method with GAT as backbone has a 8.86% gain over DGI and a 6.15% gain over GAT. On Coauthor-CS, the proposed unsupervised method shows competitive performance compared to the supervised models and performs better than DGI. On Coauthor-Phy, even with large label rate, the proposed method shows competitive performance compared to the supervised models. For the inductive learning on Coauthor-Phy, we can see both DGI and CGNN perform a bit worse than the supervised methods. This is mainly because the label rate of Coauthor-Phy is 57.98% which is quite large compared to other datasets. The supervised models will have less probability to have the over-fitting problem with a large label rate.

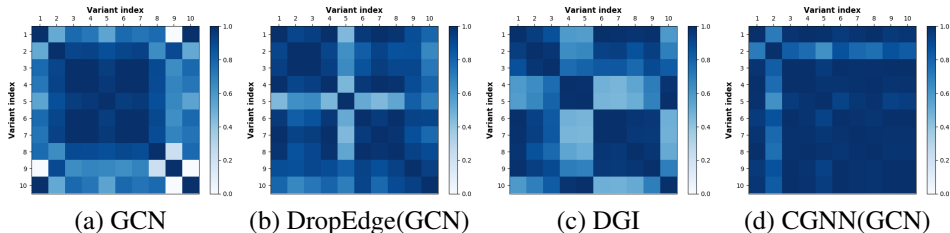


Figure 3: The representation *stability* visualization on Facebook. The mean value of the normalized cosine similarity in (a) (b) (c) (d) respectively is 0.792, 0.857, 0.804 and 0.946. Deeper color indicates larger similarity and a node representation that is more stable to slight perturbations on the input.

4.4 Representation Stability Visualization

Here we conduct an experiment to show that our method learns stable node representations on graphs. Specifically, after we train a model, we fix the model and add perturbations to the input by dropping edges with $\rho = 0.3$ 10 times. In this way, for an arbitrary node v_0 , we can have its 10 variant inputs and their corresponding 10 node representations by the fixed model. Next, we calculate the cosine similarity matrix $S \in \mathbb{R}^{10 \times 10}$ of these 10 variants' representations. If a model learns stable node

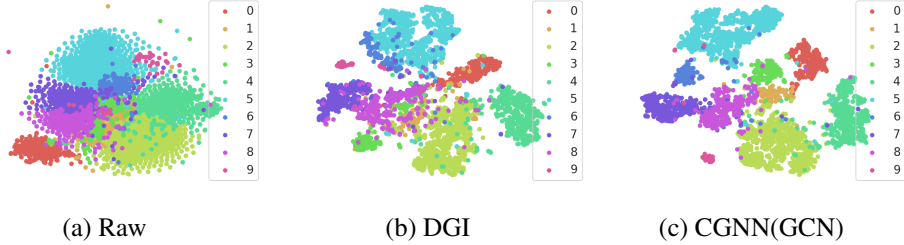


Figure 4: The t-SNE visualization of learned node representations on Coauthor-CS. Note that for clear presentation, we visualize the former ten categories of nodes. (a) Raw means the raw node features are used. (b) DGI indicates the features are learned by DGI. (c) means the features are learned by CGNN(GCN). The Silhouette score for (a) (b) (c) respectively is -0.007, 0.220 and 0.226.

representations, the similarity between each two representations should be large. Here, we randomly sample a test node and calculate the S matrix for four methods and obtain four S matrices. For better illustration, we apply min-max normalization on the four S matrices and visualize them in Figure 3.

From Figure 3, we summarize that the proposed method learns more stable node representations. Both GCN and DGI have many light-colored blocks, which means the node representation is sensitive to the slight changes on the input. Compared to GCN and DGI, DropEdge(GCN) shows a better result with deeper-colored blocks. It is because DropEdge(GCN) is trying to maintain the *stability* by assigning the same label to the input with slight perturbations. However, with the label as an agent, it is hard to guarantee the *stability* on the node representations. Instead, the proposed CGNN explicitly imposes the *stability* on the node representations. Thereby, CGNN(GCN) shows the best results, and almost all blocks in Figure 3 (d) are deep-colored.

4.5 Representation Smoothness and Identifiability Visualization

We also conduct an experiment to show the *smoothness* and *identifiability* of learned node representations. Discussing *smoothness* and *identifiability* without any data is incomprehensible. Here we use node categories to illustrate this by assuming that nodes from the same category should be clustered together (i.e. *smoothness*) and nodes from different categories should be discriminative (i.e. *identifiability*). In particular, we visualize the learned node representations on Coauthor-CS by t-SNE Maaten and Hinton [2008] in Figure 4.

From Figure 4, we can summarize that CGNN learns more clustered and discriminative node representations compared to the raw features and those learned by DGI. From Figure 4 (a), it is clear that raw features are easily overlapped together. DGI and CGNN(GCN) in Figure 4 (b) and (c) show better performance by identifying nodes from different clusters. Furthermore, CGNN(GCN) shows the most clustered and discriminative node representations. This indicates node representations from the same cluster are smooth and node representations from different clusters are distinguishable.

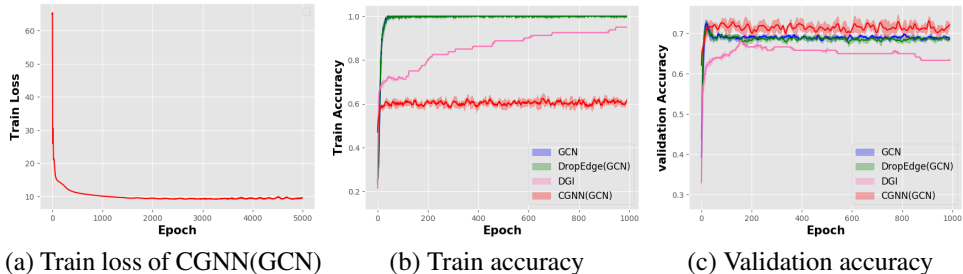


Figure 5: The effects of learned node representations on Facebook. (a) is the training loss curve. (b) indicates the train accuracy of different methods. (c) indicates the validation accuracy of different methods. For GCN and DropEdge(GCN), they are supervised methods. For DGI and CGNN(GCN), they are unsupervised methods and the accuracy curves are plot based on the one-layer linear classifier.

4.6 Effects of Learned Node Representations

We conduct an experiment to explore what are the effects of learned node representations. We show the train loss, train accuracy and validation accuracy for different methods on Facebook in Figure 5.

From Figure 5 (a), we empirically show that the proposed CGNN has obvious convergence. From Figure 5 (b) and (c), we can see that the supervised models (GCN and DropEdge) have a serve over-fitting problem. The unsupervised models DGI and CGNN do not easily overfit the data. Especially for CGNN, we can see that although it has the lowest train accuracy, it shows the best validation accuracy. It is because CGNN learns stable node representations, namely the GNN feature extractor has less variance and has better generalization ability. It is also worthwhile to point out that there are other works trying to solve the over-fitting problem on graphs Rong et al. [2019], Li et al. [2019a], Xu et al. [2018]. These methods are orthogonal to ours and we can incorporate them together. For example, we use ResGCN Li et al. [2019a] and JKNet Xu et al. [2018] as backbones and DropEdge Rong et al. [2019] as our edge dropping method. Due to limited pages, more experiments can be found in Appendix G.

5 Conclusion and Future Work

In this paper, we propose a novel method called contrastive graph neural networks (CGNN) that studies robust node representations based on sampling neighbours of nodes on graphs. CGNN is a general framework and provides a new insight for the robust design of numerous graph algorithms. By optimizing the objective in CGNN, we can learn more robust node representations that alleviate the over-fitting problem. Through extensive experiments, the effectiveness of CGNN is verified.

However, there are still some inadequacies of our method. For example, the sampling method of unpaired samples is random sampling, which would lead to the risk of sampling similar representations of the anchor node and construct wrong contrastive signals. In future, we would explore better sampling methods to construct contrastive signals with the guidance of recent works Zhen Yang [2020], Ma and Collins [2018], Chen et al. [2018, 2017].

Statement of the Potential Broader Impact: Robust node representations on graphs are useful in many applications Wang et al. [2018, 2019b], Li et al. [2019b]. For example, in e-commerce networks, robust node representations can help make recommendation for users. In some fraudulent networks, robust node representations can help recognize which users are fraudsters. Note that the constructed contrastive signals in this paper are constructed on desensitized data and will not have any privacy or ethical conflicts.

References

J. Chen, J. Zhu, and L. Song. Stochastic training of graph convolutional networks with variance reduction. *arXiv preprint arXiv:1710.10568*, 2017.

J. Chen, T. Ma, and C. Xiao. Fastgen: fast learning with graph convolutional networks via importance sampling. *arXiv preprint arXiv:1801.10247*, 2018.

F. R. Chung and F. C. Graham. *Spectral graph theory*. Number 92. American Mathematical Soc., 1997.

M. Defferrard, X. Bresson, and P. Vandergheynst. Convolutional neural networks on graphs with fast localized spectral filtering. In *Advances in neural information processing systems*, pages 3844–3852, 2016.

M. Gutmann and A. Hyvärinen. Noise-contrastive estimation: A new estimation principle for unnormalized statistical models. In *Proceedings of the Thirteenth International Conference on Artificial Intelligence and Statistics*, pages 297–304, 2010.

W. Hamilton, Z. Ying, and J. Leskovec. Inductive representation learning on large graphs. In *Advances in neural information processing systems*, pages 1024–1034, 2017.

K. He, X. Zhang, S. Ren, and J. Sun. Deep residual learning for image recognition. In *Proceedings of the IEEE conference on computer vision and pattern recognition*, pages 770–778, 2016.

G. E. Hinton, N. Srivastava, A. Krizhevsky, I. Sutskever, and R. R. Salakhutdinov. Improving neural networks by preventing co-adaptation of feature detectors. *arXiv preprint arXiv:1207.0580*, 2012.

R. D. Hjelm, A. Fedorov, S. Lavoie-Marchildon, K. Grewal, P. Bachman, A. Trischler, and Y. Bengio. Learning deep representations by mutual information estimation and maximization. *arXiv preprint arXiv:1808.06670*, 2018.

E. Hubbell, W.-M. Liu, and R. Mei. Robust estimators for expression analysis. *Bioinformatics*, 18(12):1585–1592, 2002.

T. N. Kipf and M. Welling. Semi-supervised classification with graph convolutional networks. In *International Conference on Learning Representations (ICLR)*, 2017.

G. Li, M. Muller, A. Thabet, and B. Ghanem. Deepgcns: Can gcns go as deep as cnns? In *Proceedings of the IEEE International Conference on Computer Vision*, pages 9267–9276, 2019a.

M. Li, S. Chen, X. Chen, Y. Zhang, Y. Wang, and Q. Tian. Actional-structural graph convolutional networks for skeleton-based action recognition. In *Proceedings of the IEEE Conference on Computer Vision and Pattern Recognition*, pages 3595–3603, 2019b.

Q. Li, Z. Han, and X.-M. Wu. Deeper insights into graph convolutional networks for semi-supervised learning. In *Thirty-Second AAAI Conference on Artificial Intelligence*, 2018.

Q. Li, X.-M. Wu, H. Liu, X. Zhang, and Z. Guan. Label efficient semi-supervised learning via graph filtering. In *Proceedings of the IEEE Conference on Computer Vision and Pattern Recognition*, pages 9582–9591, 2019c.

Z. Ma and M. Collins. Noise contrastive estimation and negative sampling for conditional models: Consistency and statistical efficiency. *arXiv preprint arXiv:1809.01812*, 2018.

L. v. d. Maaten and G. Hinton. Visualizing data using t-sne. *Journal of machine learning research*, 9(Nov):2579–2605, 2008.

A. Mnih and K. Kavukcuoglu. Learning word embeddings efficiently with noise-contrastive estimation. In *Advances in neural information processing systems*, pages 2265–2273, 2013.

H. NT and T. Maehara. Revisiting graph neural networks: All we have is low-pass filters. *arXiv preprint arXiv:1905.09550*, 2019.

A. v. d. Oord, Y. Li, and O. Vinyals. Representation learning with contrastive predictive coding. *arXiv preprint arXiv:1807.03748*, 2018.

B. Poole, S. Ozair, A. v. d. Oord, A. A. Alemi, and G. Tucker. On variational bounds of mutual information. *arXiv preprint arXiv:1905.06922*, 2019.

Y. Rong, W. Huang, T. Xu, and J. Huang. Dropedge: Towards deep graph convolutional networks on node classification. In *International Conference on Learning Representations*, 2019.

B. Rozemberczki, C. Allen, and R. Sarkar. Multi-scale attributed node embedding, 2019.

M. M. Saad, C. J. Bleakley, and S. Dobson. Robust high-accuracy ultrasonic range measurement system. *IEEE Transactions on Instrumentation and Measurement*, 60(10):3334–3341, 2011.

O. Shchur, M. Mumme, A. Bojchevski, and S. Günnemann. Pitfalls of graph neural network evaluation. *arXiv preprint arXiv:1811.05868*, 2018.

J. Tang, C. Aggarwal, and H. Liu. Node classification in signed social networks. In *Proceedings of the 2016 SIAM international conference on data mining*, pages 54–62. SIAM, 2016.

Y. Tian, D. Krishnan, and P. Isola. Contrastive multiview coding. *arXiv preprint arXiv:1906.05849*, 2019.

P. Veličković, G. Cucurull, A. Casanova, A. Romero, P. Liò, and Y. Bengio. Graph Attention Networks. *International Conference on Learning Representations*, 2018. URL <https://openreview.net/forum?id=rJXMPikCZ>. accepted as poster.

P. Veličković, W. Fedus, W. L. Hamilton, P. Liò, Y. Bengio, and R. D. Hjelm. Deep Graph Infomax. In *International Conference on Learning Representations*, 2019. URL <https://openreview.net/forum?id=rklz9iAcKQ>.

S. Verma and Z.-L. Zhang. Stability and generalization of graph convolutional neural networks. In *Proceedings of the 25th ACM SIGKDD International Conference on Knowledge Discovery & Data Mining*, pages 1539–1548, 2019.

H. Wang, F. Zhang, J. Wang, M. Zhao, W. Li, X. Xie, and M. Guo. Ripplenet: Propagating user preferences on the knowledge graph for recommender systems. In *Proceedings of the 27th ACM International Conference on Information and Knowledge Management*, pages 417–426, 2018.

M. Wang, L. Yu, D. Zheng, Q. Gan, Y. Gai, Z. Ye, M. Li, J. Zhou, Q. Huang, C. Ma, et al. Deep graph library: Towards efficient and scalable deep learning on graphs. *ICLR Workshop on Representation Learning on Graphs and Manifolds*, 2019a.

X. Wang, X. He, Y. Cao, M. Liu, and T.-S. Chua. Kgat: Knowledge graph attention network for recommendation. In *Proceedings of the 25th ACM SIGKDD International Conference on Knowledge Discovery & Data Mining*, pages 950–958, 2019b.

Z. Wu, Y. Xiong, S. X. Yu, and D. Lin. Unsupervised feature learning via non-parametric instance discrimination. In *Proceedings of the IEEE Conference on Computer Vision and Pattern Recognition*, pages 3733–3742, 2018.

Z. Wu, S. Pan, F. Chen, G. Long, C. Zhang, and S. Y. Philip. A comprehensive survey on graph neural networks. *IEEE Transactions on Neural Networks and Learning Systems*, 2020.

B. Xu, H. Shen, Q. Cao, K. Cen, and X. Cheng. Graph convolutional networks using heat kernel for semi-supervised learning. In *Proceedings of the 28th International Joint Conference on Artificial Intelligence*, pages 1928–1934. AAAI Press, 2019.

K. Xu, C. Li, Y. Tian, T. Sonobe, K.-i. Kawarabayashi, and S. Jegelka. Representation learning on graphs with jumping knowledge networks. *International Conference on Machine Learning (ICML)*, 2018.

R. Ying, R. He, K. Chen, P. Eksombatchai, W. L. Hamilton, and J. Leskovec. Graph convolutional neural networks for web-scale recommender systems. In *Proceedings of the 24th ACM SIGKDD International Conference on Knowledge Discovery & Data Mining*, pages 974–983, 2018.

Y. Zhang, S. Pal, M. Coates, and D. Ustebay. Bayesian graph convolutional neural networks for semi-supervised classification. In *Proceedings of the AAAI Conference on Artificial Intelligence*, volume 33, pages 5829–5836, 2019.

C. Z. H. Y. J. Z. J. T. Zhen Yang, Ming Ding. Understanding negative sampling in graph representation learning. In *Proceedings of the 26th ACM SIGKDD International Conference on Knowledge Discovery & Data Mining*, 2020.

C. Zhuang and Q. Ma. Dual graph convolutional networks for graph-based semi-supervised classification. In *Proceedings of the 2018 World Wide Web Conference*, pages 499–508, 2018.

A Proof of the Posterior Probability

Here we demonstrate the details about the derivation of the posterior in Eq. 8. To clarify this derivation, for z_0^1 , we denote z_x^2 as a variable which could either be the paired representation z_0^2 or the unpaired representation z_j^2 . Then, We define a binary latent variable c that determines whether two node representations z_0^1, z_x^2 are paired ($c = 1$) or unpaired ($c = 0$). Then, we can have:

$$p(z_0^1, z_x^2|c=1) = p_d(z_0^1, z_x^2), \quad p(z_0^1, z_x^2|c=0) = p_n(z_0^1, z_x^2) \quad (12)$$

where p_d means the data distribution and p_n indicates the noise distribution. z_0^1 has one paired node representation z_0^2 and K unpaired ones z_j^2 , thus the priors on c are:

$$p(c=1) = \frac{1}{K+1}, \quad p(c=0) = \frac{K}{K+1} \quad (13)$$

Thereby, the posterior of $c = 1$ can be written as Eq. 14 by following the Bayesian rule.

$$p(c=1|z_0^1, z_x^2) = \frac{p(z_0^1, z_x^2|c=1)p(c=1)}{p(z_0^1, z_x^2|c=0)p(c=0) + p(z_0^1, z_x^2|c=1)p(c=1)} \quad (14)$$

$$= \frac{p_d(z_0^1, z_x^2)}{p_d(z_0^1, z_x^2) + Kp_n(z_0^1, z_x^2)} \quad (15)$$

$$= \frac{p_d(z_x^2|z_0^1)}{p_d(z_x^2|z_0^1) + Kp_n(z_x^2|z_0^1)} \quad (16)$$

B Proof of Lemma 1

The derivation of Lemma 1 is derived as follows. The objective function in Eq. 3 is indeed a categorical cross-entropy that classifies the paired sample correctly. To clarify this lemma, for z_0^1 , we denote z_0^2 as a paired sample and z_j^2 as an unpaired sample. Let us write the optimal probability for minimizing \mathcal{L}_1 in Eq. 3 as $p(d=0|z_0^1, z_0^2, z_j^2|_{j=1}^K)$ where $[d=0]$ being the indicator that z_0^2 is the paired sample. Then we can have:

$$p(d=0|z_0^1, z_0^2, z_j^2|_{j=1}^K) = \frac{p(z_0^2|z_0^1) \prod_{i \neq 0} p(z_i^2)}{\sum_{j=0}^K p(z_j^2|z_0^1) \prod_{i \neq j} p(z_i^2)} \quad (17)$$

$$= \frac{\frac{p(z_0^2|z_0^1)}{p(z_0^2)}}{\sum_{j=0}^K \frac{p(z_j^2|z_0^1)}{p(z_j^2)}} \quad (18)$$

$$= \frac{\frac{p(z_0^1, z_0^2)}{p(z_0^1)p(z_0^2)}}{\sum_{j=0}^K \frac{p(z_0^1, z_j^2)}{p(z_0^1)p(z_j^2)}} \quad (19)$$

By comparing the above equation with \mathcal{L}_1 , we can see that the optimal value of $h_\theta(z_0^1, z_0^2)$ in Eq. 3 is proportional to $\frac{p(z_0^1, z_0^2)}{p(z_0^1)p(z_0^2)}$.

C Proof of the Mutual Information Lower Bound \mathcal{L}

In order to derive the mutual information lower bound \mathcal{L} , we first have the following Lemma for the score function h_ϕ :

Lemma 1 *The optimal value of score function $h_\phi(z_0^1, z_0^2)$ for minimizing loss \mathcal{L}_1 in Eq. 3 is proportional to the density ratio between the joint distribution $p(z_0^1, z_0^2)$ and the product of the marginals $p(z_0^1)p(z_0^2)$, which can be shown as follows:*

$$h_\phi(z_0^1, z_0^2) \propto \frac{p(z_0^1, z_0^2)}{p(z_0^1)p(z_0^2)} \quad (20)$$

where \propto standards for 'proportional to'. The derivation regarding this lemma is provided in Appendix B.

ALGORITHM 1: Contrastive Graph Neural Networks

Input: 1)The adjacency matrix $A \in \mathbb{R}^{N \times N}$ of graph \mathcal{G} ;
 2) A GNN backbone model f_θ ;
 3) The drop ratio ρ , the sampling size K and the temperature τ ;
Output: The node representation matrix $Z = \mathbb{R}^{N \times d}$.

while not converged **do**

drop edges
 According to Eq. 1, randomly dropping edges with a certain ratio ρ two times to obtain two different adjacent matrices A^1 and A^2 ;
 # GNN encoding
 For an arbitrary node v_0 , extracting the embeddings z_0^1 and z_0^2 of node v_0 from A^1 and A^2 , respectively;
 Randomly sampling K unpaired node embeddings of z_j^1 and z_j^2 from the memory bank;
 # contrastive learning loss
 According to Eq. 9, 10 and 11, calculating the noise contrastive loss and updating the parameters of f_θ .
 # update the memory bank
 Updating the node embeddings in the memory bank.

end

Considering Lemma 1, if we replace the score function in Eq. 3 with the density ratio in Eq. 20, we have:

$$\mathcal{L}_1 = -\mathbb{E}_{\{z_0^1, z_0^2, z_j^2 | j=1\}} \left[\log \frac{h_\phi(z_0^1, z_0^2)}{\sum_{j=0}^K h_\phi(z_0^1, z_j^2)} \right] \quad (21)$$

$$= -\mathbb{E}_{\{z_0^1, z_0^2, z_j^2 | j=1\}} \log \left[\frac{\frac{p(z_0^1, z_0^2)}{p(z_0^1)p(z_0^2)}}{\sum_{j=0}^K \frac{p(z_0^1, z_j^2)}{p(z_0^1)p(z_j^2)}} \right] \quad (22)$$

$$= \mathbb{E}_{\{z_0^1, z_0^2, z_j^2 | j=1\}} \log \left[1 + \frac{p(z_0^1)p(z_0^2)}{p(z_0^1, z_0^2)} \sum_{j=1}^K \frac{p(z_0^1, z_j^2)}{p(z_0^1)p(z_j^2)} \right] \quad (23)$$

$$= \mathbb{E}_{\{z_0^1, z_0^2\}} \log \left[1 + \frac{p(z_0^1)p(z_0^2)}{p(z_0^1, z_0^2)} K \mathbb{E}_{z_j^2} \left[\frac{p(z_0^1 | z_j^2)}{p(z_0^1)} \right] \right] \quad (24)$$

$$= \mathbb{E}_{\{z_0^1, z_0^2\}} \log \left[1 + \frac{p(z_0^1)p(z_0^2)}{p(z_0^1, z_0^2)} K \right] \quad (25)$$

$$\geq \log(K) - \mathbb{E}_{\{z_0^1, z_0^2\}} \log \left[\frac{p(z_0^1, z_0^2)}{p(z_0^1)p(z_0^2)} \right] \quad (26)$$

$$= \log(K) - \mathcal{I}(z_0^1, z_0^2) \quad (27)$$

Similarly for the loss function \mathcal{L}_2 in Eq. 5, we have:

$$\mathcal{L}_2 \geq \log(K) - \mathcal{I}(z_0^1, z_0^2) \quad (28)$$

By combining the derivation together, we have the following formulation:

$$\mathcal{I}(z_0^1, z_0^2) \geq \log(K) - \frac{1}{2}(\mathcal{L}_1 + \mathcal{L}_2) \geq \log(K) - \mathcal{L} \quad (29)$$

From Eq. 29, we can see that our contrastive objective function \mathcal{L} in Eq. 6 is the *lower bound* of the mutual information $\mathcal{I}(z_0^1, z_0^2)$.

D Algorithm Description

The concise steps of CGNN are illustrated in Algorithm 1.

E Details about Proposition 1

The details about Proposition 1 is given as follows. For clarity, we denote v_0 as an arbitrary node in graph \mathcal{G} . The randomly sampled unpaired node set of v_0 is \mathcal{K} and the similar node set of v_0 is \mathcal{M} . Therefore, the probability of sampling a node $v_j (j \neq 0)$ that belongs to \mathcal{K} is represented as:

$$P(v_j \in \mathcal{K}) = \frac{|\mathcal{K}|}{N-1} \quad (30)$$

Table 3: The hyper-parameter setting of different models on the used benchmarks. “-” indicates the number of layers is the same as the backbone model.

Model	nlayers	Hyper-parameters
GCN	2	lr:0.003, weight_decay:5e-3, dropout:0.5, n_hidden:128, iterations:1,000
ResGCN	3	lr:0.003, weight_decay:5e-3, dropout:0.5, n_hidden:128, iterations:1,000
JKNet	3	lr:0.003, weight_decay:5e-3, dropout:0.5, n_hidden:128, iterations:1,000
GraphSage	2	lr:0.01, weight_decay:5e-4, dropout:0.5, n_hidden:128, iterations:1,000
GAT	2	lr:0.005, weight_decay:5e-4, num_heads:8, num_out_heads:8, iterations:1,000
DropEdge	-	The hyper-parameters follow the settings of different backbones. The drop edge ratio is 0.3.
DGI	2	lr:0.001, weight_decay:0.0, dropout:0.0, n_hidden:512, iterations:300.
CGNN	-	lr:0.001, The other hyper-parameters follow the settings of different backbones. The drop edge ratio ρ is 0.3, the temperature τ is 0.1 and the sampling size K is 1024.

where $|\cdot|$ represents the length of a set and N is the number of nodes in graph \mathcal{G} . Similarly, the probability of sampling a node $v_j (j \neq 0)$ that belongs to \mathcal{M} is represented as:

$$P(v_j \in \mathcal{M}) = \frac{|\mathcal{M}|}{N-1} \quad (31)$$

Then, the probability of sampling a node $v_j (j \neq 0)$ that belongs to both \mathcal{K} and \mathcal{M} is represented as:

$$P(v_j \in \mathcal{K}, v_j \in \mathcal{M}) = \frac{|\mathcal{K} \cap \mathcal{M}|}{N-1} \quad (32)$$

Then the risk of sampling a similar node v_j that belongs to \mathcal{K} can be defined as the conditional probability of $v_j \in \mathcal{M}$ given $v_j \in \mathcal{K}$, which shows:

$$\mathcal{R} = P(v_j \in \mathcal{M} | v_j \in \mathcal{K}) = \frac{|\mathcal{K} \cap \mathcal{M}|}{|\mathcal{K}|} \quad (33)$$

The optimal value of Eq. 33 to maximize the mutual information with contrastive learning is 0. In practice, according to recent works Oord et al. [2018], Tian et al. [2019], the empirical value of sampling size K in contrastive learning is large (e.g. 1024, 2048, 4096) since NCE is a high biased estimator. Thereby, empirically, $|\mathcal{K}|$ can be considered as a constant around a certain value, which indicates that $|\mathcal{K} \cap \mathcal{M}|$ takes the main factor for the value of Eq. 33. We can have a low risk when \mathcal{G} has a large N and a small $|\mathcal{M}|$. In other words, a large N means we have more nodes for unpaired sampling and it is less probable to sample similar nodes belonging to unpaired nodes. A small $|\mathcal{M}|$ indicates various categories on \mathcal{G} , which also leads to a small value of $|\mathcal{K} \cap \mathcal{M}|$.

F Detailed Parameter Settings of Different Models

More detailed parameter settings are shown in Table 3. Note that for some datasets such as Pubmed and Coauthor-CS which have been reported in many works, the hyper-parameter settings are the same with the original paper or codes Kipf and Welling [2017], Wang et al. [2019b], Veličković et al. [2019], Shchur et al. [2018]. For Facebook, the above hyper-parameter settings also perform well. In order to make a fair comparison, we do not tune the hyper-parameters of different backbones for the proposed CGNN and directly use them to show the comparison results.

G More Experiments

G.1 Hyper-parameter Analysis

In the proposed method, there are three important hyper-parameters: the ratio of dropping edges ρ , the sampling size K and the temperature τ in the score function. In order to explore the effects of these hyper-parameters, we further conduct an experiment to illustrate this. The results on Pubmed are shown in Figure 6. From this figure, we can summarize that:

- In Figure 6 (a), either a too small sampling size or a too large sampling size can lead to deteriorated performance. As it is analysed in Oord et al. [2018], Tian et al. [2019], NCE is a high biased and

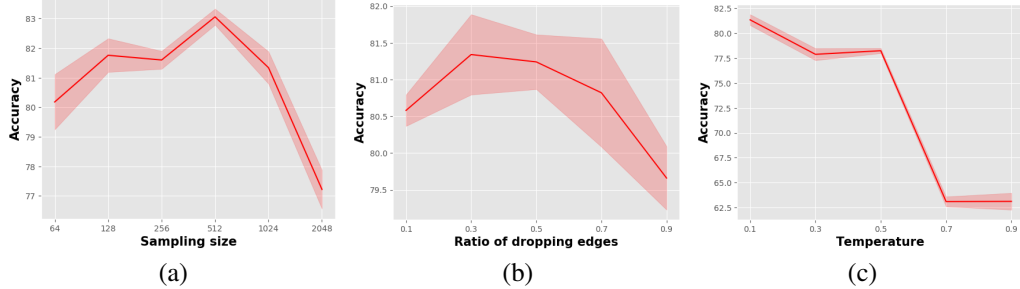


Figure 6: The effect of different hyper-parameters on Pubmed. (a) indicates the sampling size K . (b) indicates the ratio ρ of dropping edges. (c) represents the temperature τ in the score function.

low variance estimator, and it requires a large sampling size K to tighten the mutual information *lower bound*. When K is too large, according to Proposition 1, the risk of sampling similar nodes in \mathcal{K} will be enlarged. In other words, too large K can lead to inappropriate contrastive signals and deteriorates the quality of node representations. It is also worthwhile to point out that the method will show more promising results with $K = 512$ on Pubmed compared to the results with $K = 1024$ shown in Table 2.

- In Figure 6 (b), a proper drop ratio ρ tends to be around 0.5. A too small ρ leads to less variants of a node’s neighbours. A too large ρ will lose too much neighborhood information, which hinders the information propagation on graphs. It is important to point out that the smaller changes of the input data does not mean better performance because the factors leading to over-fitting in the data is data-dependent.
- The temperature τ controls the distribution of the score function. The method has its best performance when $\tau = 0.1$. Empirically, $\tau \ll 0.1$ will cause value explosion in networks because of the exponential property. In summary, $\tau = 0.1$ is an empirical value for satisfied model performance and is consistent with the choice in recent works Tian et al. [2019], Hinton et al. [2012].

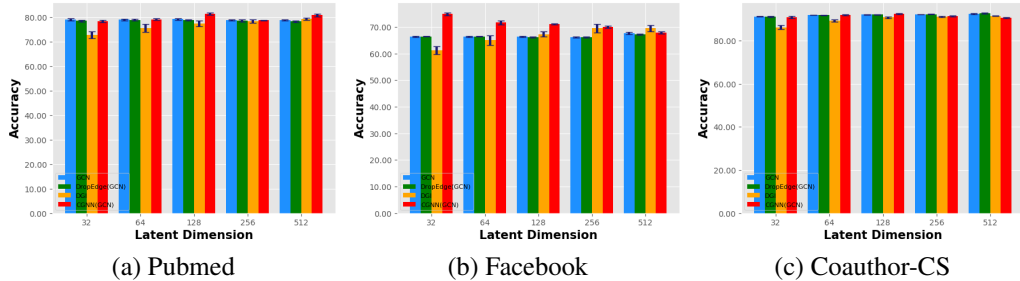


Figure 7: The effect of different latent dimensions on different benchmarks. For clarity, we show the performance of some representative methods such as GCN, DropEdge(GCN), DGI and CGNN(GCN). The standard error of each bar is also shown in this figure.

G.2 Different Latent Dimensions

For representation learning on graphs, the latent dimension is also an important factor that influences the model performance. We conduct an experiment to more comprehensively compare the performance of different methods. The results are shown in Figure 7. From this figure, we have the following observations:

- Compared to the supervised methods (i.e. GCN and DropEdge(GCN)) on different dimensions, the proposed unsupervised method CGNN(GCN) reaches competitive performance and even exceeds the supervised ones on different benchmarks.
- Compared to DGI on different dimensions, the proposed CGNN(GCN) shows better performance and *stability* on the three benchmarks. The performance of DGI varies a lot along different dimensions and has its best performance when the latent dimension is 512. By contrast, CGNN(GCN) provides more stable and better performance along different latent dimensions.